Journal Pre-proof

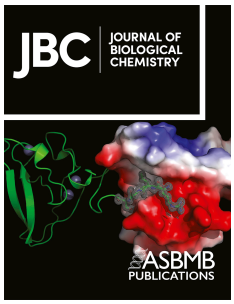

Transient Receptor Potential Vanilloid 4 in Macrophages Mediates TGF-β Activation to Drive Myofibroblast Differentiation and Pulmonary Fibrosis

Lisa M. Grove, Caitlin Snyder, Adam M. Boulton, Hongxia Mao, Susamma Abraham, Haley Ricci, Erica M. Orsini, Brian D. Southern, Mitchell A. Olman, Rachel G. Scheraga

PII: S0021-9258(26)00005-0

DOI: https://doi.org/10.1016/j.jbc.2026.111135

Reference: JBC 111135

To appear in: *Journal of Biological Chemistry*

Received Date: 10 October 2025

Revised Date: 24 December 2025

Accepted Date: 27 December 2025

Please cite this article as: Grove LM, Snyder C, Boulton AM, Mao H, Abraham S, Ricci H, Orsini EM, Southern BD, Olman MA, Scheraga RG, Transient Receptor Potential Vanilloid 4 in Macrophages Mediates TGF-β Activation to Drive Myofibroblast Differentiation and Pulmonary Fibrosis, *Journal of Biological Chemistry* (2026), doi: https://doi.org/10.1016/j.jbc.2026.111135.

Title: Transient Receptor Potential Vanilloid 4 in Macrophages Mediates TGF-β Activation to Drive Myofibroblast Differentiation and Pulmonary Fibrosis

Authors: Lisa M. Grove[1], Caitlin Snyder[1], Adam M. Boulton[1], Hongxia Mao[1], Susamma Abraham[1], Haley Ricci[1], Erica M. Orsini,[2] Brian D. Southern,[1,2] Mitchell A. Olman[1,2], Rachel G. Scheraga[1,2*]

Affiliations:

[1] Inflammation and Immunity, Cleveland Clinic Research, Cleveland Clinic

[2] Integrated Hospital Care Institute, Department of Pulmonary and Critical Care, Cleveland Clinic

* Corresponding author: Rachel G. Scheraga; 9500 Euclid Ave, Cleveland, OH 44122; Email: scherar@ccf.org

The authors have declared that no conflict of interest exists.

Abstract: Emerging evidence suggests that macrophage-fibroblast interactions can drive organ fibrosis. Myofibroblast differentiation is a key step in the pathogenesis of pulmonary fibrosis that requires both a soluble (e.g., TGF-β) and mechanical signal. We have previously implicated the fibroblast mechanosensitive cation channel, transient receptor potential vanilloid 4 (TRPV4), as a mediator of myofibroblast differentiation and experimental pulmonary fibrogenesis in response to matrix biophysical signals. Less is understood regarding how or if the matrix drives macrophage activation to mediate fibrosis. We demonstrate that loss of TRPV4 specifically in myeloid cells protects against experimental pulmonary fibrosis *in vivo*. Mechanistically, macrophage TRPV4 responds to matrix substrate stiffness in the pathophysiologic range, thereby optimizing TGF-β activation. Macrophage conditioned media transfer and coculture systems demonstrate a profound effect of TRPV4-dependent TGF-β activation in inducing myofibroblast differentiation in fibroblasts. This TGF-β activating effect was dependent on the actinomyosin binding domain within the C-terminal intracytoplasmic tail of TRPV4 and on assembly of actinomyosin cytoskeleton and its force generation. Our current study identifies a novel TRPV4-TGF-β axis in macrophages that drives myofibroblast differentiation and experimental pulmonary fibrosis through optimal activation of TGF-β. As TGF-β is a critical pro-fibrotic factor, these findings are broadly applicable to many fibrotic diseases.

One Sentence Summary: TRPV4 activates TGF-β in macrophages to drive fibrosis.

Main Text:

INTRODUCTION

Fibrotic interstitial lung diseases (fILDs) are devastating progressive disorders that carry a high mortality and lack a cure (1, 2). The hallmark of fILDs is accumulation of pathogenic fibroblasts referred to as myofibroblasts (3). Myofibroblasts have distinct pro-fibrotic characteristics including changes in motility, secretion of extracellular matrix proteins (e.g., collagen, fibronectin, and matrix components) and pro-fibrotic cytokines (e.g., TGF-β) (4). Conditions where myofibroblast development, pro-fibrotic actions, and clearance are not tightly regulated in a spatio-temporal manner leads to progressive fibrosis (5, 6). Understanding the key signals that mediate myofibroblast differentiation are essential for ameliorating fibrosis in many organs.

The myofibroblast differentiation response to extracellular matrix mechanical force is essential to the development of fibrosis. Emerging evidence suggests mechanosensitive cation channels such as Piezo 1, Piezo 2, and Transient receptor potential vanilloid 4 (TRPV4) are important in the pathogenesis of pulmonary fibrosis (7-10). Our group has specifically implicated TRPV4 in fibroblasts in TGF-β induced fibroblast to myofibroblast transdifferentiation and experimental pulmonary fibrosis (8, 9). We additionally have shown that macrophage activation also depends on matrix stiffness, an effect not recognized previously, as *in vitro* experiments were performed on supraphysiologic tissue culture plastic and glass, which have a stiffness a million times that of lung tissue (11, 12). While ubiquitously expressed, TRPV4 has been increasingly recognized to have cell-type and context-specific actions, likely as a consequence of TRPV4 crosstalk with other signaling pathways (13). This crosstalk could be mediated through TRPV4's intracytoplasmic amino- and carboxy-terminal tails or its cation channel function (14, 15).

Fibroblasts have long been identified as a key effector cell in fibrosis, whereas the contribution of immune cells has been more controversial (16-19). More recently it has been shown that alveolar macrophages persist at the leading edge of fibrosis, the fibroblastic foci, and evidence supports their important contribution to fibrogenesis, albeit through an unclear mechanism (17, 20, 21). Thus, this work was initiated to uncover previously unknown macrophage TRPV4-dependent, pro-fibrotic actions. Here, we identify TRPV4 in macrophages as a key driver of TGF-β activation that induces myofibroblast differentiation and mediates experimental pulmonary fibrosis. We found that optimal matrix substrate stiffness-dependent TGF-β activation in macrophages requires actinomyosin-induced force, and the presence of the actinomyosin binding site within TRPV4's C-terminal intracytoplasmic tail. This novel macrophage TRPV4-TGF-β axis may function as a druggable target to ameliorate organ fibrosis.

RESULTS

TRPV4 deletion in myeloid cells protects the lung from bleomycin-induced pulmonary fibrosis. To investigate the role of TRPV4 in myeloid cells on *in vivo* pulmonary fibrogenesis, the effect of 1.5 U/kg intratracheal instillation of bleomycin or saline (Day 14) was studied in myeloid specific *Trpv4* KO mice (*Trpv4*^{LysMCre}), as compared with parental controls (*Trpv4*$^{fl/fl}$). The myeloid specific *Trpv4* KO mice (*Trpv4*^{LysMCre}) were significantly protected from bleomycin-induced fibrosis (n >/= 5-20 mice per group). This was assessed by the complementary techniques of lung hydroxyproline content by >50% (**Figure 1 A**), collagen-1 levels in lung tissue by immunoblotting (**Figure 1 B**), lung compliance (**Figure 1 C)**, and representative flow-volume loop in **Supplemental Figure S 1**. Lung histologic analysis of Hematoxylin and Eosin (H&E) (**Figure 1 D**) and trichrome stained (**Figure 1 E**) lung tissue revealed more prominent fibrosis in parental controls compared to the myeloid specific *Trpv4* KO (*Trpv4*^{LysMCre}). To assess the extent of lung injury, bronchoalveolar lavage (BAL) analysis revealed decreased lymphocyte infiltration (by 25%) (**Figure 1 F**) without a change in total cell counts (data not shown), and decreased BALF total protein (by 50%) (**Figure 1 G**) in the myeloid specific *Trpv4* KO (*Trpv4*^{LysMCre}). These data collectively support the conclusion that TRPV4 in the myeloid population mediate fibrogenesis in response to bleomycin *in vivo*.

Macrophages produce a TRPV4 and matrix stiffness-dependent factor that induces myofibroblast differentiation. Since we previously published that TRPV4 can control macrophage cytokine production in response to TLR stimulation (11, 12), we now hypothesize that TRPV4 may also play a role in pro-fibrotic macrophage actions. To that end, the effect of the conditioned media from WT BMDMs and *Trpv4* KO BMDMs plated on polyacrylamide gels of varying stiffness on myofibroblast differentiation was compared. The substrate stiffnesses was

chosen in order to recapitulate that of normal (1 kPa) and fibrotic (8, 25kPa) lung, with supraphysiological tissue-culture plastic (10^6 kPa) as a positive control. The BMDM conditioned media (CM) (24 hours) was then transferred to WT mouse lung fibroblasts (MLF) which was assessed for their myofibroblast differentiation. The CM from WT BMDMs plated on 25 kPa gels and tissue-culture plastic (but not those on 1 kPa and 8 kPa gels) induced myofibroblast differentiation, as measured by staining and quantifying alpha-smooth muscle (α-SMA) actin in stress fibers (**Figure 2 A, B, Supplemental Figure S 6A**), and by immunobloting for collagen-1 in myofibroblast lysates (**Figure 2 C, D**). As evidence of the importance of TRPV4 in pro-fibrotic macrophage actions, the CM from *Trpv4* KO BMDMs did not induce myofibroblast differentiation, even with supraphysiologic substrate stiffness (**Figure 2 A-D**). These data indicate that a TRPV4 and matrix-stiffness dependent, soluble factor is produced by macrophages that drives myofibroblast differentiation.

TGF-β is the profibrotic factor in conditioned media that induces myofibroblast differentiation. As macrophages can produce TGF-β (20, 22-27), we next tested if TGF-β from macrophages induces myofibroblast differentiation, using complementary techniques. The effect of the TGF-β receptor kinase inhibitor, SD208, on myofibroblast differentiation was measured upon incubation of fibroblasts with CM from WT BMDM that were plated on various stiffnesses. The stiffness-mediated profibrotic effect of macrophage CM as described above, is abrogated upon treatment of the fibroblasts with SD208 (**Figure 3 A, B, Supplemental Figure S 6B**). As TGF-β initiates complex canonical and non-canonical intracellular signals (28, 29), we examined the role of the canonical TGF-β pathway by downregulating SMAD proteins. SMAD3 siRNA downregulated SMAD3 protein (by approximately 71-76%; **Supplemental Figure S 2A and 2B**) and blocked the capacity of WT BMDM CM to induce myofibroblast differentiation in

fibroblasts, compared to non-targeting siRNA (**Supplemental Figure S 2A-D**). These data demonstrate that WT BMDM conditioned media initiates canonical TGF-β intracellular signals. In order to definitively demonstrate that TGF-β is the predominant TRPV4 and stiffness-dependent pro-fibrotic factor, the effect of either neutralization or immunodepletion of WT BMDM conditioned media on myofibroblast differentiation was determined. Neutralization or immunodepletion of TGF-β using an affinity purified polyclonal antibody reduced the TGF-β in the WT BMDM CM by ~80% and decreased myofibroblast differentiation by 50-100% compared with that from isotype control antibody (**Figure 3 C-E, Supplemental Figure S 6C**). Taken together, these data strongly indicate that TGF-β from macrophages initiated canonical TGF-β signaling in a TRPV4 and matrix-stiffness dependent manner, that drives myofibroblast differentiation of fibroblasts.

***Trpv4* KO macrophages have impaired TGF-β activation.** As data reveals that TGF-β is the predominant soluble factor secreted by macrophages that drives myofibroblast differentiation, we determined the antigenic level of TGF-β in the WT and *Trpv4* KO BMDM CM. Surprisingly, total antigenic TGF-β levels were similar and independent of substrate stiffness in the WT and *Trpv4* KO BMDMs (**Figure 4 A**). In order to resolve the apparent divergent results of immunodepletion/Smad3 signaling findings with that of equal TGF-β abundance (**Figure 3 D, E**), we determined the level of TGF-β activation using a mink lung epithelial TGF-β reporter cells (MLEC) as described (30, 31). WT BMDM CM has more active TGF-β, and the active/total TGF-β ratio was significantly higher in WT vs *Trpv4* KO BMDM CM (**Figure 4 B**).

As cell-cell contact is known to robustly activate TGF-β through cellular force mechanisms (31, 32), we compared the TGF-β activation level and myofibroblast differentiating effect using

macrophage-fibroblast coculture systems. Coculture with *Trpv4* KO BMDM decreased the number of myofibroblasts by approximately 42% as compared to WT BMDM (**Figure 4 C, D, Supplemental Figure S 6D**), further supporting the conclusion that TRPV4 in BMDMs drives myofibroblast differentiation that is more pronounced upon coculture than media transfer experiments **as in Figure 2**. The extent of the difference in the TRPV4-dependent TGF-β activation capacity of monolayers was approximately half of that of the coculture system, supporting previous work of the dependency of cell-cell contact on TGF-β activation (**Figure 4 E, F; Supplemental Figure S 3**).

Activation of TGF-β by TRPV4 depends on actinomyosin cytoskeleton function. We previously published that TRPV4 activity potentiates TGF-β1–induced actomyosin remodeling in fibroblasts (9). To that end, we determined the effect of inhibiting actinomyosin stability and function on macrophage activation of TGF-β and the myofibroblast differentiating capacity of the macrophage conditioned media. Cytochalasin D (destabilizes actin) and jaksplakinolide (blocks actin turnover) decreased the activation of TGF-β (**Figures 5 A, B**) without a change in total TGF-β (**Supplemental Figure S 4A-D**) (33, 34). As myosin binds actin fibers to generate force (35), we tested the effect of blebbistatin, a myosin II ATP-ase inhibitor, on TGF-β activating capacity of WT BMDM. Similarly, blebbistatin reduced the TGF-β activating capacity without affecting its secretion (**Figure 5 C; Supplemental Figure S 4E, F**). Importantly, blebbistatin treatment of WT BMDMs reduced their capacity to induce myofibroblast differentiation to the level of *Trpv4* KO BMDMs while having no effect on the myofibroblast differentiation capacity of the *Trpv4* KO BMDMs (**Figure 5 D, E, Supplemental Figure S 6E**). These latter findings suggest that the entirety of the TRPV4 effect is a consequence of its capacity to regulate cytoskeletal stability. Together, these data implicate the critical role for the

actinomyosin cytoskeleton in responding to TRPV4 initiated signals to activate TGF-β and drive myofibroblast differentiation.

Activation of TGF-β is dependent on the C-terminal domain, actinomyosin binding region on TRPV4. Given our finding of the importance of the actinomyosin cytoskeletal function and known binding of the C-terminal intracellular tail to actinomyosin (36), we determined the effect of deletion/mutation of the TRPV4 actinomyosin binding domain/site (C-terminal domain deletion AA 723-871) on its capacity to activate TGF-β and drive myofibroblast differentiation. Lentiviral mediated expression of a TRPV4 mutant lacking its C-terminal domain resulted in a suppression of TGF-β activation and myofibroblast differentiation to the level of untransduced or control vector-transduced *Trpv4* KO BMDMs (**Figure 6 A-E, Supplemental Figure S 6F**). The transfection efficiency of the FL and Cdel TRPV4 LV were relatively equal, as measured by immunoblot (**Supplemental Figure S 5**).

To further substantiate the importance of actinomyosin binding to the TRPV4 C-terminal domain, we tested the effect of expression of a TRPV4 actinomyosin binding site specific scrambled mutant (AA 746-779) on the macrophages' capacity to activate TGF-β (37). Similarly, expression of the actinomyosin specific mutant (AM LV) in the *Trpv4* KO BMDMs demonstrated an impaired capacity (~30%) to activate TGF-β compared to that of FL TRPV4 (**Figure 6 F**), despite relatively equal transduction/expression efficiency (**Supplemental Figure S 5**). These data provide further evidence for the importance of TRPV4-actinomyosin binding site in mediating TGF-β activation and myofibroblast differentiation. Taking collectively with the presented *in vitro* and *in vivo* data, we convincingly demonstrate that TRPV4's actinomyosin

binding function drives TGF-β activation, myofibroblast differentiation, and experimental pulmonary fibrosis.

DISCUSSION

Our foundational work shows that the mechanosensitive, cation ion channel, TRPV4, plays a key role in myofibroblast differentiation, *in vivo* pulmonary fibrosis, and the macrophage response to infection (8, 9, 11, 12). The current work seeks to determine if TRPV4 in macrophages mediates the pro-fibrotic pathway through paracrine signaling to fibroblasts and if so through what molecular mechanism. Collectively, the data presented here show that macrophage TRPV4 is required to secrete a pro-fibrotic factor that leads to myofibroblast differentiation and collagen-1 production (**Figure 7**). As TGF-β is a cytokine or growth factor that is pro-fibrotic, our data supports that the TRPV4-dependent pro-fibrotic factor produced by the macrophage is TGF-β. Although TRPV4 didn't play a role in secretion of TGF-β as levels were equal in WT and *Trpv4* KO macrophages, TRPV4 is required for the optimal activation of TGF-β. Furthermore, activation of TGF-β by macrophages requires TRPV4's C-terminal actinomyosin binding domain along with an intact and functional actinomyosin cytoskeleton. Taken together, this work demonstrates the novel TRPV4-TGF-β axis whereby the C-terminal actinomyosin binding domain of TRPV4 in macrophages is required for force-dependent activation of TGF-β resulting in myofibroblast differentiation and experimental pulmonary fibrosis.

The etiology of fILDs, especially those related to connective tissue diseases, have been shown to be driven in part by immune mechanisms (1). Yet more recently, even the idiopathic form, idiopathic pulmonary fibrosis (IPF), has also been shown to involve both the innate (macrophages, neutrophils) and adaptive (T cells) immune system (16, 17). Specifically, several lines of evidence support that macrophages play a role in fibrogenesis such as *i)* unique subsets of pro-fibrotic macrophages are found on single-cell RNA sequencing of fibrotic human and mouse lung tissue, *ii)* macrophages are a primary source of active TGF-β, and *iii)* macrophage

depletion protects against fibrosis, but the mechanism of the macrophage induction of fibrosis is not clearly defined (17, 20, 22-27, 38). IPF pathogenesis is known to involve, among other processes, epithelial injury, immune cell infiltration, and fibroblast-to-myofibroblast transition driving extracellular matrix (ECM) deposition and pro-fibrotic cytokine production (e.g., TGF-β) (32, 39-42). This leads to tissue stiffening, and recruitment of monocyte-derived macrophages (MDM), thereby establishing a self-perpetuating cycle of fibrotic foci formation, a hallmark of IPF (20, 22, 43-46).

Single cell RNA sequencing (scRNAseq) of animal and human BAL, and samples from fibrotic lung tissue reveal distinct monocyte-derived macrophages and alveolar macrophage populations with pro-fibrotic features (24-27). Specifically, TRPV4 is highly upregulated in macrophages from IPF patients as shown in scRNAseq data from the human IPF lung atlas (47). Lung macrophage phenotype varies based on their ontogeny, location in the lung, and their surrounding microenvironment (48, 49). However, how the lung microenvironment affects the phenotype of macrophages has been less explored. The lung microenvironment changes during the aging process, which leads to many chronic lung diseases, such as IPF and senescence-associated secretory phenotype (SASP) (50, 51). In fact, aging leads to changes in the matrix biophysical properties and components, and in quantity and function of macrophage populations, similar to that seen in IPF (52-54). Emerging data suggests that the lung macrophage phenotype is plastic and comprises a pro-fibrotic "M2-like" population is responsible for TGF-β production and secretion (22). Our data demonstrates that TRPV4 shifts the macrophage population towards a pro-fibrotic, TGF-β activating phenotype in response to matrix mechanical stiffness in the pathophysiologic range, as seen in IPF. This study only used bone marrow-derived macrophages differentiated with M-CSF (50 ng/ml, 7 days). Future work will determine the pro-fibrotic effect

of TRPV4 in the alveolar versus interstitial macrophage given they interact with different aspects of the lung microenvironment. Parenthetically, in other work we have published there was no difference in the TRPV4 dependence of the LPS response in BMDMs and alveolar macrophages from mice and humans (11, 12).

TGF-β is a unique cytokine as it is secreted in its inactive form and can be activated, in part, through several mechanical force dependent mechanisms (55). The inactive or latent form of TGF-β is in a trimeric complex with the latent TGF-β binding proteins (LTBPs) and latent TGF-β prodomain (LAP) (56). LTBPs are known to bind fibronectin and fibrillin, which sequesters the TGF-β-LAP complex into the extracellular matrix, thereby localizing TGF-β activity (57-59). In turn, integrins in the β1 (αvβ3 and αvβ6) and β2 (like αMβ2 or Mac-1) family can bind the Arg-Gly-Asp (RGD) integrin-specific binding motif in the LAP (18, 28). Cell-cell or cell-matrix force can facilitate conformational change of the TGF-β-LAP complex exposing active TGF-β to its cognate receptor in order to initiate intracellular signaling (59-61). Our work supports cytoskeletal binding to TRPV4's C-terminal actinomyosin domain, which is the initiating event that is suggested to result in force generation leading to TGF-β activation by monocyte-derived macrophages. TRPV4 can control cytoskeletal-induced force through several possible mechanisms. TRPV4 may affect integrin function directly by facilitating integrin binding to the LAP RGD domain, as TRPV4 is needed for the β1 integrin functions of cell matrix adhesion, cytoskeletal organization and integrin to integrin signaling in other cell types (62, 63). Alternatively, the TRPV4 dependency on Glycoprotein A repetitions predominant (GARP) function, TGF-β-LAP activating and signaling receptor, on immune cells such as macrophages and T cells, has yet to be explored (64, 65). The literature supports that cells in contact with each other activate more TGF-β than those that are not in contact (60). As our data

shows that TRPV4 binds to the cytoskeleton via its C-terminal tail to generate force, we hypothesize that the *Trpv4* KO BMDMs would not generate as much force on cell-cell contact, lessening the macrophage's capacity to expose the cryptic TGF-β receptor binding site of the latent TGF-β complex (29, 60). This would result in an impaired ability of the latent TGF-β complex to bind to its nascent receptor as evident by the impaired measured TGF-β activation. Other possibilities include potential differences in integrin binding or in other cell adhesion proteins such as connexin or cadherins between the WT and *Trpv4* KO BMDMs (31, 60, 61).

Interestingly, our data shows that loss of TRPV4 induces a small change in TGF-β activation as compared to the large protection from both myofibroblast differentiation and experimental pulmonary fibrosis (**Figures 1, 2 and 4**). One potential explanation is that the myofibroblast differentiation response to TGF-β in not linear and is quite variable in different cells and systems (66-68). For example, if the cell is stimulated with a small amount of active TGF-β but over a prolonged period of time, there may be a longer lasting pro-fibrotic effect (67, 68). The consequences of linearity and exposure time are not considered in our *in vitro* experimental system. Nonetheless, we saw a clear *in vivo* effect that mimicked our *in vitro* findings. There is a possibility that this *in vivo* effect may also be due to TRPV4 deletion in a portion type II alveolar epithelial cells (AEC) that may be affected by the LysMCre promoter (69). Both murine and human epithelial cells have been shown to activate TGF-β (60). However, we show, using multiple techniques, that CM from WT BMDMs alone can induce myofibroblast differentiation and collagen-1 production (**Figure 2**) due to active TGF-β (**Figure 4**), and these functions are significantly decreased with TRPV4 deletion (**Figures 2 and 4**). Although we saw abrogation of the myofibroblast differentiation effect with neutralizing TGF-β, it remains possible that there is an additional TRPV4-dependent macrophage factor that is synergistic with

TGF-β's pro-fibrotic actions, such as platelet-derived growth factor (PDGF) and Wnt signaling (66, 68, 70, 71). Other putative TRPV4 and stiffness-dependent pro-fibrotic factors will be investigated in the future.

Taken together, our work advances the understanding of the mechanism of TGF-β activation by macrophages that leads to myofibroblast differentiation and pulmonary fibrosis. A strength of our observations is that complementary gain and loss of function and molecular antibody based, and overexpression systems reveal similar results. However, there are some limitations to the methodology and interpretations of our study. All of our data is using mouse *in vitro* and *in vivo* systems that may exhibit different biologic response than humans. However, this is somewhat mitigated by the fact that IPF macrophages exhibit high levels of TRPV4 and TGF-β. Although we have solid evidence of the existence of a macrophage-TRPV4-cytoskeleton-TGF-β activating axis, other previously described mechanisms exist for activation of TGF-β (18). Even though calmodulin, a cytoskeleton activating protein, is known to bind to the intracellular C-terminal domain of TRPV4, its site of binding is distinct from that of the actinomyosin binding domain (72). Furthermore, the level of impairment of TGF-β activation among the TRPV4 actinomyosin scrambled mutant and C-terminal deleted mutant is similar. These data suggest that the calcium-dependent calmodulin binding to TRPV4 is not a significant contributor to the overall results. Calcium signaling has been shown to be indirectly involved in TGF-β activation (73). However, it is experimentally difficult to discern if either TRPV4-dependent calcium function or other macrophage calcium channels play a major role in our findings, due to the protean effects of intracellular calcium on general macrophage function.

In conclusion, fibrosis is a consequence of multiple coordinated biological processes. Pulmonary fibrosis requires both a mechanical and soluble signal. We have previously shown

that TRPV4 is essential for *in vivo* pulmonary fibrosis and the macrophage response to infection using global *Trpv4* KO mice. The data presented herein demonstrates that macrophage TRPV4 is a key effector in the fibrosis process by optimally activating TGF-β, thereby driving myofibroblast differentiation and experimental pulmonary fibrosis. The TRPV4 function is dependent on the presence of the actinomyosin binding domain on its C-terminal intracellular tail and on an intact and functioning cytoskeleton. Targeting TGF-β directly has been unsuccessful likely given its pleotropic effects (19). We speculate that focusing on localized macrophage TRPV4-dependent activation of TGF-β may elicit a more favorable response and therefore may serve as a druggable target in the treatment of pulmonary fibrosis.

MATERIALS AND METHODS

Sex as a biological variable

Both male and female BMDMs and transgenic mice were used in this study.

Antibodies and reagents

Blebbistatin, jaksplakinolide, cytochalastin D, ALK5 inhibitor (SD208), and antibodies to alpha smooth muscle actin and collagen-1 were from Sigma Aldrich. Alexa Fluor 594-phalloidin and Alexa Fluor-conjugated secondary antibodies were from Invitrogen. Antibody to GAPDH was obtained from Fitzgerald, glass-bottom or plastic plates containing activated polyacrylamide gels of 1, 8, or 25kPa were custom made by Matrigen Life Technologies. Mink lung epithelial TGF-β reporter cells (MLEC) were a gift from Dr. Raed Dweik. The TGF-β ELISA was purchased from R&D systems, as was the TGF-β antibody used for pull-down and neutralization. Smad and TRPV4 antibodies were purchased from Cell Signaling, and the siRNA was from Dharmacon. The Isotype control antibody for pull-down and neutralization experiments was from Biolegend. TRPV4 full-length, C-terminal deleted, and actinomyosin mutant lentivirus were purchased from VectorBuilder. In order to generate an actomyosin binding-deficient construct we mutated the nucleic acid sequence of TRPV4 corresponding to amino acids 746 to 779 (RSFPVFLRKAFRSGEMVTVGKSSDGTPDRRWCFR). We mutated these 34 amino acids to a 17 X GS repeat in order to maintain proper structure of the carboxy-terminal tail of TRPV4 and conserve all other functions. C57BL/6 mice were from The Jackson Laboratory. *Trpv4* KO mice were a gift from David Zhang.

Bleomycin-induced pulmonary fibrosis model

Induction of pulmonary fibrosis was performed in a single dose bleomycin model in *Trpv4*$^{fl/fl}$ and *Trpv4*^{LysMCre} mice generated by us. Bleomycin (1.5U/kg) or phosphate-buffered saline (as a control) was instilled intratracheally as previously published (9). Animals were euthanized at 14 days after bleomycin and left lung collected for hydroxyproline (a marker of collagen deposition) and collagen-1 by immunoblot (9). Right lungs were inflated with OCT as previously published (9). Static compliance, elastance, and resistance measurements were performed on the FlexiVent animal ventilator (Scireq). Anesthetized, tracheostomized, paralyzed, and mechanically ventilated mice were used to perform P-V loop measurements, to obtain lung compliance. Bronchoalveolar lavage was performed to determine total cell counts and differentials and total protein as a marker of vascular leak as described previously (9, 11). All animal protocols were performed according to guidelines approved by the Cleveland Clinic Institutional Animal Care and Use Committee (IACUC).

Cell culture, conditioned media transfer, and immunoblotting

Primary mouse lung fibroblasts (MLFs) were derived from 7- to 10-week-old WT mice and propagated in complete media (MEM supplemented with 10% fetal bovine serum (FBS)) as previously described (9, 74). MLFs were obtained by outgrowth of fragments of collagenase digested lung tissue as we published (9). MLF media was changed every 2-3 days and MLF were passaged with trypsin-EDTA when the cells reached 80-90% confluence, for up to five passages (74). WT MLFs were cultured the same way on tissue culture plastic (without polyacrylamide gels) and pretreated ± ALK5 inhibitor (SD208) or SMAD2/SMAD3 siRNA for experiments with WT CM added to fibroblasts, or in coculture with bone marrow derived macrophages (BMDMs). Primary BMDMs were harvested from 8–12-week-old WT or *Trpv4* KO mice and maintained in

10% FBS/RPMI. BMDMs were differentiated in recombinant mouse macrophage colony stimulating factor (MCSF, 50 ng/ml, Peptrotech) as previously published.(11, 12) BMDMs were plated in 10% FBS/RPMI on tissue culture plastic or on plastic plates containing polyacrylamide gels of 1, 8, or 25 kPa. Then, the BMDMs were pretreated ± blebbistatin, jaksplakinolide, or cytochalasin D for 24h, then the conditioned media was removed and analyzed for total TGF-β (ELISA), active TGF-β (MLEC – see below), or for its ability to induce myofibroblast differentiation in WT MLFs. The BMDM conditioned media (CM) was subjected to ± TGF-β neutralization with TGF-β antibody or immunodepletion using a bead-based assay (or isotype control),(75-77) was then added to the WT MLFs (1:10 in 1% BSA/SFM-MEM) for 48h, and myofibroblast differentiation was read out by immunofluorescence (below) or by Western blotting for collagen-1 (below).

The BMDMs were cultured on fibronectin-coated (10 μg/ml) polyacrylamide hydrogels of indicated stiffnesses. The conditioned media from these BMDMs was then transferred to fibroblasts that were plated on tissue culture plastic. For BMDM/MLF coculture assays (**Figures 4C-4E**), BMDMs and MLFs were mixed prior to plating on tissue culture plastic in 10% SCM overnight in macrophage medium. The next day the BMDM/MLF cocultures were washed 2 times in SFM, and 1% BSA/SFM was added for 48 hours, after which the CM was harvested and analyzed, and cocultures were stained (as below). For BMDM/MLEC coculture assays (**Supplemental Figure S3**), BMDMs and MLEC were mixed prior to plating on tissue culture plastic in 10% SCM overnight in macrophage culture media (RPMI 10% FBS). The next day the coculture CM was harvested and analyzed for total TGF-β by ELISA. The MLECs were washed and lysed for luminescence assays for active TGF-β, as below.

Immunofluorescence/Immunoblotting

Immunoblotting was performed as previously published. For collagen-1, GAPDH, SMAD2 and SMAD3 detection in WT MLF, cells were lysed in 1% NP-40 lysis buffer and separated on Criterion gels (Biorad) at a constant 100V and transferred to 0.45-micron PVDF membranes (Thermo Scientific) at a constant 100mA for 2 hours. For TRPV4 full length and mutant lentivirus detection in transfected BMDMS, TRPV4 antibody (LSBio) was used with the same protocol. Primary and HRP-tagged secondary antibodies were used as published and detected using an enhanced chemiluminescence system (Amersham ECL Prime Western Blotting Detection Reagent) on a UVP Biospectrum imaging system (Analytik Jena) using total time image integration as published (9, 11, 12). Band density was quantified using VisionWorks acquisition and analysis software version 8.19.17027.9424 (Analytik Jena) and normalized to GAPDH in each lane. Regarding antibody validation, the collagen-1 and GAPDH antibodies used within have been previously published by our lab (8, 9, 78), the SMAD2 and SMAD 3 band densities were significantly decreased with their respective siRNAs, and the TRPV4 antibody band size was specific for the mutant molecular weights.

To determine the BMDM CM effect on myofibroblast differentiation in WT MLF, WT MLF were treated as in the previous section, fixed in 4% paraformaldehyde, permeabilized with 0.5% Triton X-100, and blocked with 2% normal goat serum. To label SMA, primary SMA antibody (1:1000) was used, followed by AlexaFluor488 secondary (1:1000). F-actin stress fibers were stained by AlexaFluor 594 phalloidin (1:100). Images were acquired using a Leica DM IRB inverted microscope (Leica Microsystems) equipped with a Leica DFC 7000T camera and Leica Application Suite X (LAS X) v.3.6.0.20104 software.

411 WT MLF were considered myofibroblasts if the SMA and F-actin were aligned in stress fibers –
412 and at least 30 cells/condition were counted in duplicate wells. Regarding antibody validation,
413 the SMA, F-actin (phalloidin), and secondary antibodies used within have been previously
414 published by our lab (8, 9, 78).
415
416 **TGF-β Activity Assay**
417 Active TGF-β was determined via mink lung epithelial cells (MLEC), which make luciferase in
418 response to active TGF-β via the plasminogen activator inhibitor-1 (PAI-1) promoter (79).
419 BMDM CM (from 500,000 BMDM/ml) was added directly to attached MLEC for 20 hours, or,
420 for coculture experiments, MLEC and BMDM were plated directly together for 20 hours.
421 MLECs were lysed, and luminescence was determined with a luciferase assay kit (Promega) and
422 luminometer (SpectraMax iD3, Molecular Devices, Softmax Pro Software 7.0.3).
423
424 **siRNA mediated knockdown**
425 All siRNAs were transfected into WT MLFs using siLentFect lipid reagent (Bio-Rad) according
426 to the manufacturer's instructions. SMAD2- or SMAD3-specific siRNA and control scrambled
427 siRNA duplexes were purchased from Dharmacon and used at the indicated concentrations (24
428 hours of transfection). After transfection, cells were washed with serum-free medium (SFM) and
429 conditioned media from WT or *Trpv4* KO BMDMs were added.
430
431 **Lentiviral constructs**
432 Lentiviral constructs for (myc)–tagged wild-type TRPV4 (full length) and myc-C-terminal
433 deleted TRPV4 (Cdel, AAs 723-871 deleted) were produced by Vector Builder. The TRPV4 actin

binding site was published by Goswami et al.(37) For transduction, *Trpv4* KO BMDMs were exposed to 50 MOI of one of the above lentiviral constructs (or a control lentivirus) for 48 hours in complete RPMI supplemented with polybrene (4 μg/ml, Santa Cruz Biotechnology) as published.(80) Cells were washed three times with SFM and transferred to 1% BSA/SFM for 24 hours. The BMDM conditioned media was saved and analyzed for active and total TGF-β, and the BMDMs were lysed in 1% NP-40 lysis buffer and Western-blotted for TRPV4 protein as above. Transfection efficiency was determined by Western blotting for TRPV4 and GAPDH.

Statistical analysis

All data are expressed as means ± SD unless otherwise indicated. Statistical comparisons between control and experimental groups were performed using SigmaPlot software. Student's *t* test was used for two-group comparisons, whereas one-way analysis of variance (ANOVA) was used for comparisons between more than two groups. A Student-Newman-Keuls, Tukey's test, Holm-Šídák, or Fisher's Least Significant Difference test was used to adjust for multiple comparisons. Values of $P \leq 0.05$ were considered statistically significant.

Study Approval

The animal studies were performed with approval by the Cleveland Clinic's Institutional Animal Care and Use Committee (IACUC) #2624, expiration date 03/31/2027.

Data Availability

All data from this manuscript are within the main text or supplement. The Raw data will be made available upon request.

457

458 **Author Contributions**

459 Designing research studies: LMG, MAO, RGS

460 Conducting experiments: LMG, CS, AMB, HM, SA, EMO, BDS, RGS

461 Acquiring data: LMG, CS, RGS

462 Analyzing data: LMG, CS, MAO, RGS

463 Providing Reagents: MAO, RGS

464 Writing and editing the manuscript: LMG, RGS, MAO

465

466 **Acknowledgements**: We acknowledge Dr. Dan Culver for critically reading our manuscript.

467

468 **Funding sources:**

469 National Institutes of Health grant R01-HL155064 (RGS)

470 National Institutes of Health grant R01-HL158746 (MAO)

471 National Institutes of Health grant R01-HL133721 (MAO)

472

Figure Legends:

Figure 1: TRPV4 deletion from myeloid cells protects the lung from pulmonary fibrosis.

Trpv4$^{fl/fl}$ and *Trpv4*^{LysMCre} mice were intratracheally instilled with saline (hashed bars) or 1.5 U/kg bleomycin (solid bars) and all analysis at Day 14. **A.** Hydroxyproline content increased in the lungs after bleomycin of *Trpv4*$^{fl/fl}$ as compared to *Trpv4*^{LysMCre} mice. Results shown as mean ± SD for 4 independent experiments with 22-28 mice/group (shown as individual points). $^{**}p<0.01$ *Trpv4*$^{fl/fl}$ vs *Trpv4*^{LysMCre} mice (unpaired, 2-tailed t-test). **B.** Collagen-1:GAPDH was measured in pooled whole lung homogenate from saline and bleomycin treated *Trpv4*$^{fl/fl}$ and *Trpv4*^{LysMCre} mice. Results shown as mean ± SD for 3 independent experiments (shown as individual points) with 22-28 mice/group pooled lysate. $^{*}p<0.05$ *Trpv4*$^{fl/fl}$ vs *Trpv4*^{LysMCre} mice (unpaired, 2-tailed t-test). **C.** Lung Compliance (Cst; mL/cmH20) was measured using FlexiVent. Results shown as mean ± SD for 4 independent experiments with 6-11 mice/group (shown as individual points). $^{**}p<0.01$ ± bleomycin *Trpv4*$^{fl/fl}$ (ANOVA/Holm-Sidak's multiple comparisons test). **D.** Representative photomicrographs of Hematoxylin and Eosin (H&E)-stained lung tissue from saline and bleomycin treated *Trpv4*$^{fl/fl}$ and *Trpv4*^{LysMCre} mice. Scale bar 2mm (zoomed out) and 200µm (zoomed in). **E.** Representative photomicrographs of Trichrome-stained lung tissue from saline and bleomycin treated *Trpv4*$^{fl/fl}$ and *Trpv4*^{LysMCre} mice. Scale bar 2mm (zoomed out) and 200µm (zoomed in). **F.** BALF cell differentials were measured from both genotypes with increased lymphocytes in *Trpv4*$^{fl/fl}$ mice treated with bleomycin. Results shown as mean ± SD for 4 independent experiments with 7-16 mice/group (shown as individual points). $^{***}p<0.001$ ± bleomycin *Trpv4*$^{fl/fl}$, $^{****}p<0.0001$ *Trpv4*$^{fl/fl}$ vs *Trpv4*^{LysMCre}(ANOVA/Fisher's LSD). **G.** Total protein increased in BALF in *Trpv4*$^{fl/fl}$ as compared to *Trpv4*^{LysMCre} mice. Results shown as mean

± SD for 4 independent experiments with 5-13 mice/group (shown as individual points).

**$p<0.01$ ± bleomycin *Trpv4*$^{fl/fl}$(ANOVA/Fisher's LSD).

Figure 2: TRPV4 in macrophages is required for secretion of a stiffness-dependent, pro-fibrotic factor that induces myofibroblast differentiation. Bone marrow derived macrophages (BMDMs) from WT and *Trpv4* KO mice were differentiated with M-CSF for 7 days, plated on pathophysiologic range matrix stiffnesses (1 kPa: normal lung, red bar; 8 kPa: fibrotic lung, orange bar; 25 kPa: fibrotic lung, yellow bar; Polystyrene (10^6 kPa) standard culture conditions, green bar), and conditioned media (CM) was transferred to WT mouse lung fibroblasts (MLFs). **A.** CM from WT BMDMs induced myofibroblasts in MLFs in a stiffness-dependent manner, an effect lost upon deletion of TRPV4 in macrophages as measured by immunofluorescence and quantified in **B.** Results shown as mean ± SD from 5 independent experiments (shown in individual data points) performed in technical duplicates. ***p<0.001 WT 1kPa and 8kPa vs WT 25kPa and polystyrene; $^{\#\#\#}p$<0.001 WT 25kPa and polystyrene vs KO 25kPa and polystyrene (ANOVA/Student-Newman-Keuls). Scale bar 100μm, 10x original mag. Green = alpha smooth muscle actin, red = phalloidin (F-actin), yellow = merged. **C.** CM from WT BMDMs induced collagen-1:GAPDH production in MLFs in a stiffness-dependent manner, an effect lost upon deletion of TRPV4 in macrophages as measured by immunoblot and quantified in **D.** Results shown as mean ± SEM from 4 independent experiments. WT 1kPa and *Trpv4* KO 1kPa each set to 1. **p<0.01 or *p<0.05 WT vs *Trpv4* KO on higher stiffnesses (ANOVA/Fisher's LSD).

Figure 3: TGF-β is the matrix stiffness-dependent pro-fibrotic factor secreted by macrophages. CM from differentiated WT BMDMs that were plated on pathophysiologic range matrix stiffnesses was transferred to WT MLFs ± TGF-β receptor (ALK5) inhibitor (SD208). **A.** SD208 blocked WT BMDM CM's ability to induce myofibroblasts in a stiffness-dependent manner as assessed by immunofluorescence and quantified in **B.** Results shown as mean ± SD from 3 independent experiments (shown in individual data points) performed in technical duplicates. ***p<0.001 WT 1kPa and 8kPa vs WT 25kPa and polystyrene with bar color as in Figure 2, $^{###}$p<0.001 WT 25kPa and polystyrene ± SD208 (ANOVA/Student-Newman-Keuls). Scale bar 100μm, 10x original magnification. Green = alpha smooth muscle actin, red = phalloidin, yellow = merged. **C.** Total TGF-β levels were significantly decreased with TGF-β immunodepletion or neutralization. Isotype control: blue bar, anti-TGF-β: brown bar. Results shown as mean ± SD from 3 independent experiments (shown in individual data points) performed in technical duplicates. ***p<0.001 anti-TGF-β vs isotype control (ANOVA/Student-Newman-Keuls). **D.** TGF-β neutralization or immunodepletion decreased the ability of WT BMDM CM to induce myofibroblast differentiation in MLF by immunofluorescence as quantified in **E.** Unconditioned media was set to 100%. Unconditioned media: beige bar, CM- no depletion: green bar, CM- 20μg control Ab: blue bar; CM- 20μg TGF-β Ab: brown bar. Results shown as mean ± SD from 3 independent experiments (shown in individual data points) performed in technical duplicates. *p<0.05 control vs TGF-β immunodepletion, ***p<0.001 control vs TGF-β neutralization (ANOVA/Student-Newman-Keuls). Scale bar 100mm, 20x original magnification, colors as in **A.**

Figure 4: TRPV4 in macrophages is required for optimal TGF-β activation either in monolayers or coculture with fibroblasts. A. Total TGF-β was measured from CM from WT and *Trpv4* KO BMDMs plated on pathophysiologic range matrix stiffnesses by ELISA. Results shown as mean ± SD from 5 independent experiments (individual points shown) in technical duplicates. **B.** Active TGF-β was measured upon transfer of CM from WT and KO BMDMs to MLECs by luminescence, total TGF-β was measured by ELISA. Results shown as mean ± SD from 5 independent experiments in technical duplicates (individual points shown). ****p<0.0001 WT BMDM CM vs KO BMDM CM (unpaired 2-tailed t-test). **C.** BMDMs from WT and *Trpv4* KO were mixed with WT MLFs and cocultured together for 48 hours. Myofibroblasts per field (n=3 independent experiments, 12 and 11 total fields for WT and *Trpv4* KO, respectively) were determined by immunofluorescence as quantified in **D.** Results shown as mean ± SD from 3 independent experiments in at least technical triplicates (individual points shown). ***p<0.001WT vs *Trpv4* KO BMDMs (unpaired 2-tailed t-test). Scale bar 100μm, 10x original magnification. Green = alpha smooth muscle actin, Red = phalloidin. **E.** Active and total TGF-β were measured by transferring CM from WT MLF + WT or *Trpv4* KO BMDM coculture on PS to MLEC or ELISA, respectively. Results shown as mean ± SD from 4 independent experiments in technical duplicates (individual points shown). ****p<0.0001 WT BMDM + MLF vs KO BMDM + MLF (unpaired 2-tailed t-test). **F.** Percent difference in *Trpv4* KO relative to WT for CM from BMDM alone or in coculture with WT fibroblasts. Results shown as mean ± SD from at least 4 independent experiments in technical duplicates (individual points shown). *p<0.05 BMDM CM vs coculture CM (unpaired 2-tailed t-test).

564

Figure 5: TRPV4 mediates actinomyosin-dependent TGF-β activation in macrophages to drive myofibroblast differentiation. CM from differentiated WT and *Trpv4* KO BMDMs were treated ± **A.** cytochalasin D (cyto D; 5uM), **B.** Jaksplakinolide (JAK; 0.1 μM), or **C.** blebbistatin (Bleb, 10 μM). Active TGF-β was measured upon transfer of CM to MLEC. Results shown as mean ± SD from three independent experiments (shown in individual data points) in technical duplicates. ***$p<0.001$ No cyto D vs + cyto D *$p<0.05$ WT no Bleb or no JAK vs + Bleb or JAK (unpaired 2-tailed t-test). **D.** Myofibroblast differentiation in WT MLFs treated with WT BMDM CM ± bleb was read out by immunofluorescence as quantified in **E.** Results shown as mean ± SD from three independent experiments (shown in individual data points) in technical duplicates. ***$p<0.001$ +WT bleb vs WT no bleb (ANOVA, Tukey's multiple comparisons). Scale bar 100μm, 10x original magnification. Green = alpha smooth muscle actin, red = phalloidin, yellow = merged.

Figure 6: Deletion of TRPV4's intracellular C-terminal domain (site of actin and myosin binding) inhibits TGF-β activation and myofibroblast differentiation. CM from differentiated WT and *Trpv4* KO BMDMs were treated with myc-tagged EV, FL *TRPV4*, or C-terminal deleted (Cdel) *TRPV4* lentiviral vectors. **A.** Active TGF-β was measured upon transfer of CM from WT and KO BMDMs ± LV constructs to MLEC by luminescence (WT No LV: white bar, KO No LV: red bar, KO FL TRPV4 LV: green, KO TRPV4 Cdel LV: yellow). Results shown as mean ± SD from three independent experiments (individual points shown) in technical duplicates. ***p*<0.01 KO FL TRPV4 LV vs KO no LV, **p*<0.05 KO FL TRPV4 LV vs KO Cdel LV (ANOVA/Sidak's multiple comparisons). **B.** Total TGF-β on CM was measured by ELISA. Results shown as mean ± SD from three independent experiments (individual points shown) in technical duplicates. **p*<0.05 KO no LV vs KO TRPV4 Cdel LV (bar color per A, ANOVA/Sidak's multiple comparisons). **C.** Values obtained from A and B were used to calculate Active/Total TGF-β. Results shown as mean ± SD from three independent experiments (individual points shown) in technical duplicates. ***p*<0.01 KO no LV vs FL TRPV4 LV, **p*<0.05 KO FL TRPV4 LV vs KO Cdel LV (bar color per **A**, ANOVA/Sidak's multiple comparisons). **D.** CM from WT and *Trpv4* KO BMDMs treated with EV, FL *TRPV4* or Cdel *TRPV4* was added to WT MLFs and myofibroblast differentiation was read out by immunofluorescence as quantified in **E.** Results shown as mean ± SD from three independent experiments (individual points shown) in technical duplicates. **p*<0.05 control (CNTRL) LV vs FL TRPV4 LV or KO Cdel LV (No LV: white bar, CNTRL LV: red bar, FL TRPV4 LV: green bar, TRPV4 Cdel LV: yellow bar (ANOVA/Sidak's multiple comparisons). Scale bar 100μm, 20x original magnification. Green = alpha smooth muscle actin, Red = phalloidin, Yellow = merged. **F.** CM from *Trpv4* KO BMDM treated with FL TRPV4 or TRPV4 actin binding site mutant

(AM) was analyzed for active/total TGF-β. Results shown as mean ± SD from five independent experiments in technical duplicates (individual points shown) $**p<0.01$ FL TRPV4 LV vs TRPV4 actin mutant (AM) LV (unpaired 2-tailed t-test).

607 **Figure 7: Working model of TRPV4-dependent TGF-β activation upon macrophage-**
608 **fibroblast interaction.** Upon macrophage sensing of matrix stiffness, TRPV4 C-terminal
609 domain binds to actinomyosin, thereby generating force on the integrin. Based on extensive
610 literature the integrin binds to the latency associated peptide (LAP) within the latent TGF-β
611 complex, thereby exposing the cryptic TGF-β receptor binding site. The active TGF-β binds to
612 the TGF-β receptor on the fibroblast to enhance collagen production, myofibroblast
613 differentiation and ultimately pulmonary fibrosis.
614
615
616

References:

1. Kamiya M, Carter H, Espindola MS, Doyle TJ, Lee JS, Merriam LT, et al. Immune mechanisms in fibrotic interstitial lung disease. *Cell.* 2024;187(14):3506-30.
2. Zeng Q, and Jiang D. Global trends of interstitial lung diseases from 1990 to 2019: an age–period–cohort study based on the Global Burden of Disease study 2019, and projections until 2030. *Frontiers in Medicine.* 2023;10.
3. Darby IA, Zakuan N, Billet F, and Desmoulière A. The myofibroblast, a key cell in normal and pathological tissue repair. *Cell Mol Life Sci.* 2016;73(6):1145-57.
4. Darby IA, and Hewitson TD. Fibroblast differentiation in wound healing and fibrosis. *Int Rev Cytol.* 2007;257:143-79.
5. Kendall RT, and Feghali-Bostwick CA. Fibroblasts in fibrosis: novel roles and mediators. *Front Pharmacol.* 2014;5:123.
6. Humphrey JD, Dufresne ER, and Schwartz MA. Mechanotransduction and extracellular matrix homeostasis. *Nat Rev Mol Cell Biol.* 2014;15(12):802-12.
7. Liu X, Niu W, Zhao S, Zhang W, Zhao Y, and Li J. Piezo1 ： the potential new therapeutic target for fibrotic diseases. *Progress in Biophysics and Molecular Biology.* 2023;184:42-9.
8. Grove LM, Mohan ML, Abraham S, Scheraga RG, Southern BD, Crish JF, et al. Translocation of TRPV4-PI3Kγ complexes to the plasma membrane drives myofibroblast transdifferentiation. *Sci Signal.* 2019;12(607).
9. Rahaman SO, Grove LM, Paruchuri S, Southern BD, Abraham S, Niese KA, et al. TRPV4 mediates myofibroblast differentiation and pulmonary fibrosis in mice. *J Clin Invest.* 2014;124(12):5225-38.

10. Freeberg MAT, Camus SV, Robila V, Perelas A, Thatcher TH, and Sime PJ. Piezo2 Is a key mechanoreceptor in lung fibrosis that drives myofibroblast differentiation. *Am J Pathol.* 2025;195(4):626-38.

11. Scheraga RG, Abraham S, Grove LM, Southern BD, Crish JF, Perelas A, et al. TRPV4 protects the lung from bacterial pneumonia via MAPK molecular pathway switching. *The Journal of Immunology.* 2020;204(5):1310-21.

12. Scheraga RG, Abraham S, Niese KA, Southern BD, Grove LM, Hite RD, et al. TRPV4 mechanosensitive ion channel regulates lipopolysaccharide-stimulated macrophage phagocytosis. *The Journal of Immunology.* 2016;196(1):428-36.

13. Lapajne L, Rudzitis CN, Cullimore B, Ryskamp D, Lakk M, Redmon SN, et al. TRPV4: Cell type-specific activation, regulation and function in the vertebrate eye. *Curr Top Membr.* 2022;89:189-219.

14. Parthasarathy A, Anishkin A, Xie Y, Drachuk K, Nishijma Y, Fang J, et al. Phosphorylation of distal C-terminal residues promotes TRPV4 channel activation in response to arachidonic acid. *Journal of Biological Chemistry.* 2025;301(3):108260.

15. Jiang D, Guo R, Dai R, Knoedler S, Tao J, Machens H-G, et al. The multifaceted functions of TRPV4 and calcium oscillations in tissue repair. *International Journal of Molecular Sciences.* 2024;25(2):1179.

16. Meyer KC. Immunosuppressive agents and interstitial lung disease: what are the risks? *Expert Rev Respir Med.* 2014;8(3):263-6.

17. Kolahian S, Fernandez IE, Eickelberg O, and Hartl D. Immune mechanisms in pumonary fibrosis. *American Journal of Respiratory Cell and Molecular Biology.* 2016;55(3):309-22.

18. Biernacka A, Dobaczewski M, and Frangogiannis NG. TGF-β signaling in fibrosis. *Growth Factors.* 2011;29(5):196-202.

19. Yue X, Shan B, and Lasky JA. TGF-β: Titan of lung fibrogenesis. *Curr Enzym Inhib.* 2010;6(2).

20. Misharin AV, Morales-Nebreda L, Reyfman PA, Cuda CM, Walter JM, McQuattie-Pimentel AC, et al. Monocyte-derived alveolar macrophages drive lung fibrosis and persist in the lung over the life span. *J Exp Med.* 2017;214(8):2387-404.

21. Novak CM, Sethuraman S, Luikart KL, Reader BF, Wheat JS, Whitson B, et al. Alveolar macrophages drive lung fibroblast function in cocultures of IPF and normal patient samples. *Am J Physiol Lung Cell Mol Physiol.* 2023;324(4):L507-l20.

22. McCubbrey AL, Barthel L, Mohning MP, Redente EF, Mould KJ, Thomas SM, et al. Deletion of c-FLIP from CD11bhi Macrophages Prevents Development of Bleomycin-induced Lung Fibrosis. *American Journal of Respiratory Cell and Molecular Biology.* 2018;58(1):66-78.

23. Joshi N, Watanabe S, Verma R, Jablonski RP, Chen CI, Cheresh P, et al. A spatially restricted fibrotic niche in pulmonary fibrosis is sustained by M-CSF/M-CSFR signalling in monocyte-derived alveolar macrophages. *Eur Respir J.* 2020;55(1).

24. Aran D, Looney AP, Liu L, Wu E, Fong V, Hsu A, et al. Reference-based analysis of lung single-cell sequencing reveals a transitional profibrotic macrophage. *Nature Immunology.* 2019;20(2):163-72.

25. Fastrès A, Pirottin D, Fievez L, Tutunaru AC, Bolen G, Merveille AC, et al. Identification of pro-fibrotic macrophage populations by single-cell transcriptomic analysis in west

highland white terriers affected with canine idiopathic pulmonary fibrosis. *Front Immunol.* 2020;11:611749.

26. Bhattacharya M, and Ramachandran P. Immunology of human fibrosis. *Nat Immunol.* 2023;24(9):1423-33.

27. Unterman A, Zhao AY, Neumark N, Schupp JC, Ahangari F, Cosme C, et al. Single-cell profiling reveals immune aberrations in progressive idiopathic pulmonary fibrosis. *American Journal of Respiratory and Critical Care Medicine.* 2024;210(4):484-96.

28. Deng Z, Fan T, Xiao C, Tian H, Zheng Y, Li C, et al. TGF-β signaling in health, disease and therapeutics. *Signal Transduction and Targeted Therapy.* 2024;9(1):61.

29. Massagué J, and Sheppard D. TGF-b; signaling in health and disease. *Cell.* 2023;186(19):4007-37.

30. Abe M, Harpel JG, Metz CN, Nunes I, Loskutoff DJ, and Rifkin DB. An assay for transforming growth factor-beta using cells transfected with a plasminogen activator inhibitor-1 promoter-luciferase construct. *Anal Biochem.* 1994;216(2):276-84.

31. Wipff P-J, Rifkin DB, Meister J-J, and Hinz B. Myofibroblast contraction activates latent TGF-β1 from the extracellular matrix. *Journal of Cell Biology.* 2007;179(6):1311-23.

32. Hinz B. Mechanical aspects of lung fibrosis: a spotlight on the myofibroblast. *Proc Am Thorac Soc.* 2012;9(3):137-47.

33. Bubb MR, Spector I, Beyer BB, and Fosen KM. Effects of jasplakinolide on the kinetics of actin polymerization: an explanation for certain in vivo observations *Journal of Biological Chemistry.* 2000;275(7):5163-70.

34. Casella JF, Flanagan MD, and Lin S. Cytochalasin D inhibits actin polymerization and induces depolymerization of actin filaments formed during platelet shape change. *Nature.* 1981;293(5830):302-5.

35. Squire J. Special Issue: The actin-myosin interaction in muscle: background and overview. *Int J Mol Sci.* 2019;20(22).

36. McGowan TA, Madesh M, Zhu Y, Wang L, Russo M, Deelman L, et al. TGF-beta-induced Ca(2+) influx involves the type III IP(3) receptor and regulates actin cytoskeleton. *Am J Physiol Renal Physiol.* 2002;282(5):F910-20.

37. Goswami C, Kuhn J, Heppenstall PA, and Hucho T. Importance of non-selective cation channel TRPV4 interaction with cytoskeleton and their reciprocal regulations in cultured cells. *PLoS One.* 2010;5(7):e11654.

38. Xu Y, Ying L, Lang JK, Hinz B, and Zhao R. Modeling mechanical activation of macrophages during pulmonary fibrogenesis for targeted anti-fibrosis therapy. *Science Advances.* 2024;10(13):eadj9559.

39. Wilson MS, and Wynn TA. Pulmonary fibrosis: pathogenesis, etiology and regulation. *Mucosal Immunology.* 2009;2(2):103-21.

40. Ortiz-Zapater E, Signes-Costa J, Montero P, and Roger I. Lung fibrosis and fibrosis in the lungs: is it all about myofibroblasts? *Biomedicines.* 2022;10(6).

41. Ju X, Wang K, Wang C, Zeng C, Wang Y, and Yu J. Regulation of myofibroblast dedifferentiation in pulmonary fibrosis. *Respiratory Research.* 2024;25(1):284.

42. Conte E. Targeting monocytes/macrophages in fibrosis and cancer diseases: Therapeutic approaches. *Pharmacology & Therapeutics.* 2022;234:108031.

43. Parker MW, Rossi D, Peterson M, Smith K, Sikström K, White ES, et al. Fibrotic extracellular matrix activates a profibrotic positive feedback loop. *J Clin Invest.* 2014;124(4):1622-35.

44. Hardie WD, Glasser SW, and Hagood JS. Emerging concepts in the pathogenesis of lung fibrosis. *Am J Pathol.* 2009;175(1):3-16.

45. Buechler MB, Fu W, and Turley SJ. Fibroblast-macrophage reciprocal interactions in health, fibrosis, and cancer. *Immunity.* 2021;54(5):903-15.

46. Lodyga M, Cambridge E, Karvonen HM, Pakshir P, Wu B, Boo S, et al. Cadherin-11–mediated adhesion of macrophages to myofibroblasts establishes a profibrotic niche of active TGF-β. *Science Signaling.* 2019;12(564):eaao3469.

47. Neumark N, Cosme C, Rose K-A, and Kaminski N. The Idiopathic Pulmonary Fibrosis Cell Atlas. *American Journal of Physiology-Lung Cellular and Molecular Physiology.* 2020;319(6):L887-L92.

48. Mould KJ, Barthel L, Mohning MP, Thomas SM, McCubbrey AL, Danhorn T, et al. Cell origin dictates programming of resident versus recruited macrophages during acute lung injury. *American Journal of Respiratory Cell and Molecular Biology.* 2017;57(3):294-306.

49. Mould KJ, Jackson ND, Henson PM, Seibold M, and Janssen WJ. Single cell RNA sequencing identifies unique inflammatory airspace macrophage subsets. *JCI insight.* 2019;4(5):e126556.

50. Selman M, Buendía-Roldán I, and Pardo A. Aging and pulmonary fibrosis. *Rev Invest Clin.* 2016;68(2):75-83.

51. Bahram Yazdroudi F, and Malek A. Reducing M2 macrophage in lung fibrosis by controlling anti-M1 agent. *Scientific Reports.* 2025;15(1):4120.

52. Jin J, Li L, and Fu C. Age-induced changes in lung microenvironment: from melanoma dormancy to outgrowth. *Signal Transduction and Targeted Therapy.* 2023;8(1):33.

53. Wang Y, Huang X, Luo G, Xu Y, Deng X, Lin Y, et al. The aging lung: microenvironment, mechanisms, and diseases. *Front Immunol.* 2024;15:1383503.

54. Ulldemolins A, Narciso M, Sanz-Fraile H, Otero J, Farré R, Gavara N, et al. Effects of aging on the biomechanical properties of the lung extracellular matrix: dependence on tissular stretch. *Frontiers in Cell and Developmental Biology.* 2024;Volume 12 - 2024.

55. Annes JP, Chen Y, Munger JS, and Rifkin DB. Integrin alphaVbeta6-mediated activation of latent TGF-beta requires the latent TGF-beta binding protein-1. *J Cell Biol.* 2004;165(5):723-34.

56. Robertson IB, Horiguchi M, Zilberberg L, Dabovic B, Hadjiolova K, and Rifkin DB. Latent TGF-β-binding proteins. *Matrix Biol.* 2015;47:44-53.

57. Saharinen J, Hyytiäinen M, Taipale J, and Keski-Oja J. Latent transforming growth factor-beta binding proteins (LTBPs)--structural extracellular matrix proteins for targeting TGF-beta action. *Cytokine Growth Factor Rev.* 1999;10(2):99-117.

58. Dallas SL, Sivakumar P, Jones CJ, Chen Q, Peters DM, Mosher DF, et al. Fibronectin regulates latent transforming growth factor-beta (TGF beta) by controlling matrix assembly of latent TGF beta-binding protein-1. *J Biol Chem.* 2005;280(19):18871-80.

59. Massam-Wu T, Chiu M, Choudhury R, Chaudhry SS, Baldwin AK, McGovern A, et al. Assembly of fibrillin microfibrils governs extracellular deposition of latent TGF beta. *J Cell Sci.* 2010;123(Pt 17):3006-18.

60. Munger JS, Huang X, Kawakatsu H, Griffiths MJ, Dalton SL, Wu J, et al. The integrin alpha v beta 6 binds and activates latent TGF beta 1: a mechanism for regulating pulmonary inflammation and fibrosis. *Cell.* 1999;96(3):319-28.

61. Munger JS, Harpel JG, Giancotti FG, and Rifkin DB. Interactions between growth factors and integrins: latent forms of transforming growth factor-beta are ligands for the integrin alphavbeta1. *Mol Biol Cell.* 1998;9(9):2627-38.

62. Ji C, Wang Y, Wang Q, Wang A, Ali A, and McCulloch CA. TRPV4 regulates β1 integrin-mediated cell-matrix adhesions and collagen remodeling. *Faseb j.* 2023;37(6):e22946.

63. Thodeti CK, Matthews B, Ravi A, Mammoto A, Ghosh K, Bracha AL, et al. TRPV4 channels mediate cyclic strain-induced endothelial cell reorientation through integrin-to-integrin signaling. *Circ Res.* 2009;104(9):1123-30.

64. Marcelo KL, Ribar T, Means CR, Tsimelzon A, Stevens RD, Ilkayeva O, et al. Research resource: roles for calcium/calmodulin-dependent protein kinase kinase 2 (CaMKK2) in systems metabolism. *Mol Endocrinol.* 2016;30(5):557-72.

65. Zhang M, Pan X, Fujiwara K, Jurcak N, Muth S, Zhou J, et al. Pancreatic cancer cells render tumor-associated macrophages metabolically reprogrammed by a GARP and DNA methylation-mediated mechanism. *Signal Transduct Target Ther.* 2021;6(1):366.

66. Taber A, Konecny A, Oda SK, Scott-Browne J, and Prlic M. TGF-β broadly modifies rather than specifically suppresses reactivated memory CD8 T cells in a dose-dependent manner. *Proceedings of the National Academy of Sciences.* 2023;120(48):e2313228120.

67. Rojas A, Padidam M, Cress D, and Grady WM. TGF-β receptor levels regulate the specificity of signaling pathway activation and biological effects of TGF-β. *Biochimica et Biophysica Acta (BBA) - Molecular Cell Research.* 2009;1793(7):1165-73.

68. Duan D, and Derynck R. Transforming growth factor-β (TGF-β)-induced up-regulation of TGF-β receptors at the cell surface amplifies the TGF-β response. *J Biol Chem.* 2019;294(21):8490-504.

69. McCubbrey AL, Allison KC, Lee-Sherick AB, Jakubzick CV, and Janssen WJ. Promoter specificity and efficacy in conditional and inducible transgenic targeting of lung macrophages. *Frontiers in Immunology.* 2017;Volume 8 - 2017.

70. Spanjer AI, Baarsma HA, Oostenbrink LM, Jansen SR, Kuipers CC, Lindner M, et al. TGF-β-induced profibrotic signaling is regulated in part by the WNT receptor Frizzled-8. *Faseb j.* 2016;30(5):1823-35.

71. Bahram Yazdroudi F, and Malek A. Optimal controlling of anti-TGF-beta and anti-PDGF medicines for preventing pulmonary fibrosis. *Scientific Reports.* 2023;13(1):15073.

72. Lei L, Cao X, Yang F, Shi DJ, Tang YQ, Zheng J, et al. A TRPV4 channel C-terminal folding recognition domain critical for trafficking and function. *J Biol Chem.* 2013;288(15):10427-39.

73. Shi M, Zhu J, Wang R, Chen X, Mi L, Walz T, et al. Latent TGF-β structure and activation. *Nature.* 2011;474(7351):343-9.

74. McIntosh JC, Hagood JS, Richardson TL, and Simecka JW. Thy1 (+) and (-) lung fibrosis subpopulations in LEW and F344 rats. *Eur Respir J.* 1994;7(12):2131-8.

75. Bismar H, Klöppinger T, Schuster EM, Balbach S, Diel I, Ziegler R, et al. Transforming growth factor β (TGF-β) levels in the conditioned media of human bone cells: relationship to donor age, bone volume, and concentration of TGF-β in human bone matrix in vivo. *Bone.* 1999;24(6):565-9.

76. Oida T, and Weiner HL. Depletion of TGF-β from fetal bovine serum. *J Immunol Methods.* 2010;362(1-2):195-8.

77. Jurukovski V, Dabovic B, Todorovic V, Chen Y, and Rifkin DB. Methods for measuring TGF-b using antibodies, cells, and mice. *Methods Mol Med.* 2005;117:161-75.

78. Southern BD, Li H, Mao H, Crish JF, Grove LM, Scheraga RG, et al. A novel mechanoeffector role of fibroblast S100A4 in myofibroblast transdifferentiation and fibrosis. *J Biol Chem.* 2024;300(1):105530.

79. Abe M, Harpel JG, Metz CN, Nunes I, Loskutoff DJ, and Rifkin DB. An assay for transforming growth factor-β using cells transfected with a plasminogen activator inhibitor-1 promoter-luciferase construct. *Analytical Biochemistry.* 1994;216(2):276-84.

80. Orsini EM, Roychowdhury S, Gangadhariah M, Cross E, Abraham S, Reinhardt A, et al. TRPV4 regulates the macrophage metabolic response to limit sepsis-induced lung injury. *Am J Respir Cell Mol Biol.* 2024;70(6):457-67.

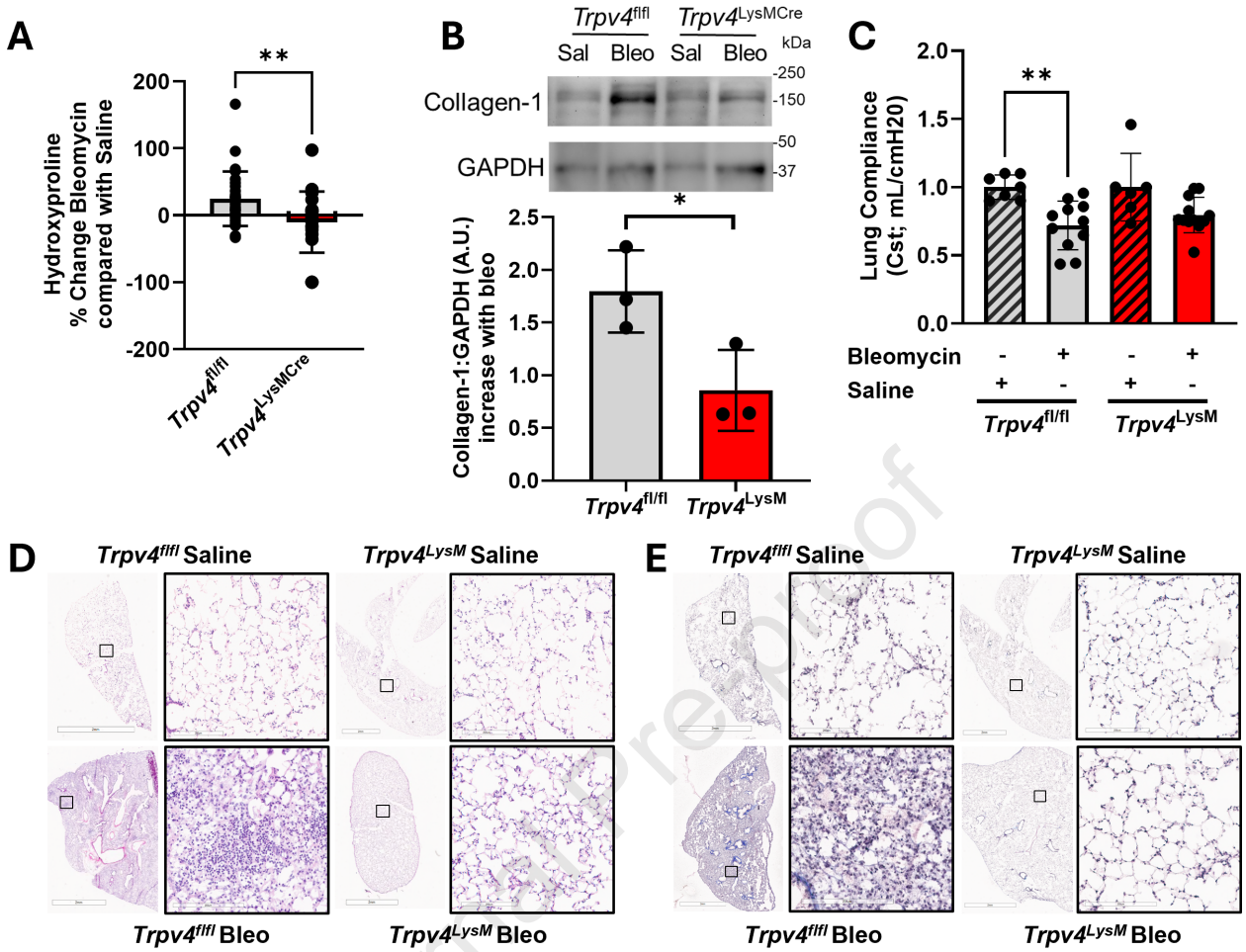
A
Hydroxyproline % Change Bleomycin compared with Saline
200
100
0
-100
-200
**
Trpv4fl/fl
Trpv4LysMCre
B
Trpv4fl/fl
Trpv4LysMCre
Sal
Bleo
Sal
Bleo
kDa
Collagen-1
GAPDH
-250
-150
-50
-37
Collagen-1:GAPDH (A.U.) increase with bleo
2.5
2.0
1.5
1.0
0.5
0.0
*
Trpv4fl/fl
Trpv4LysM
C
Lung Compliance (Cst; mL/cmH20)
2.0
1.5
1.0
0.5
0.0
**
Bleomycin
Saline
Trpv4fl/fl
Trpv4LysM
D
Trpv4flfl Saline
Trpv4LysM Saline
Trpv4flfl Bleo
Trpv4LysM Bleo
E
Trpv4flfl Saline
Trpv4LysM Saline
Trpv4flfl Bleo
Trpv4LysM Bleo
F
BALF % Cell Differential
150
100
50
0
-50
***
****
Bleomycin
Saline
Trpv4fl/fl
Trpv4LysM
Trpv4fl/fl
Trpv4LysM
Macrophages
Lymphocytes
G
BALF Protein
2000
1500
1000
500
0
**
Bleomycin
Saline
Trpv4fl/fl
Trpv4LysM

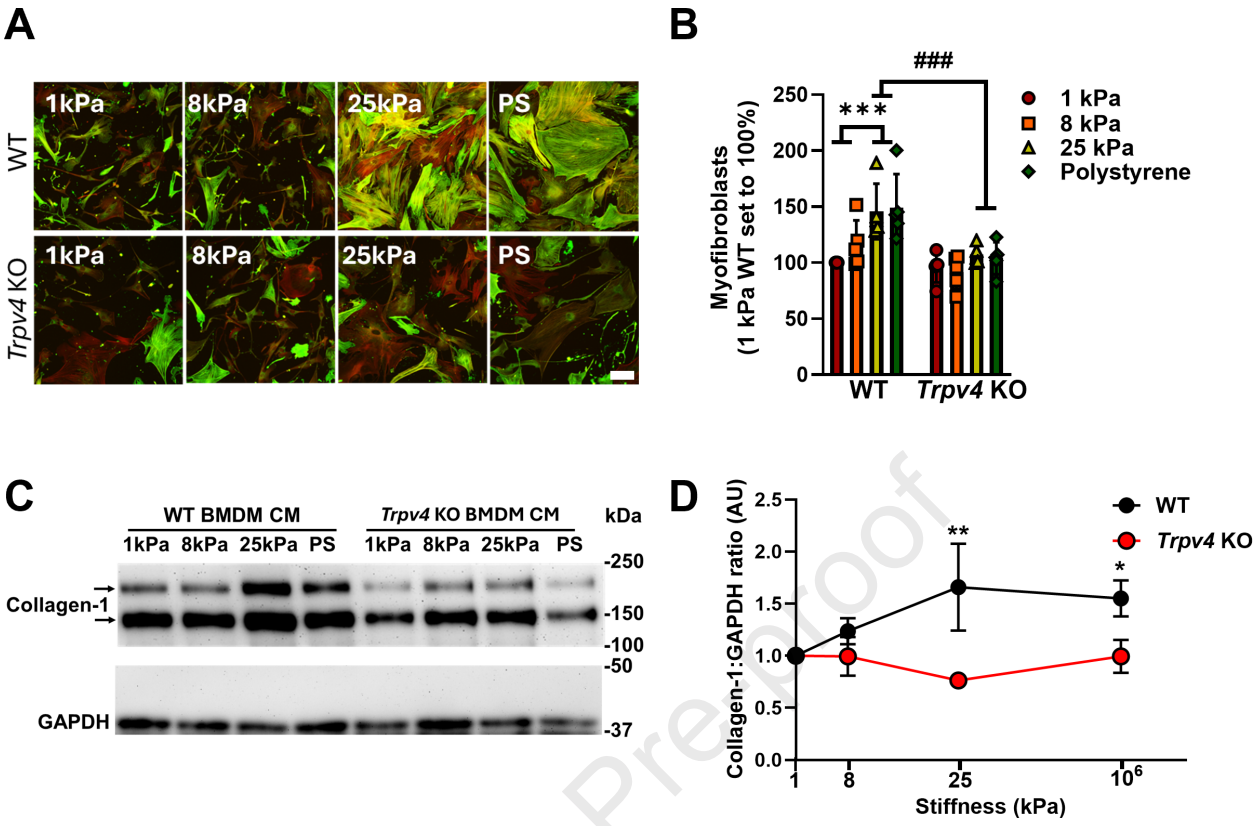

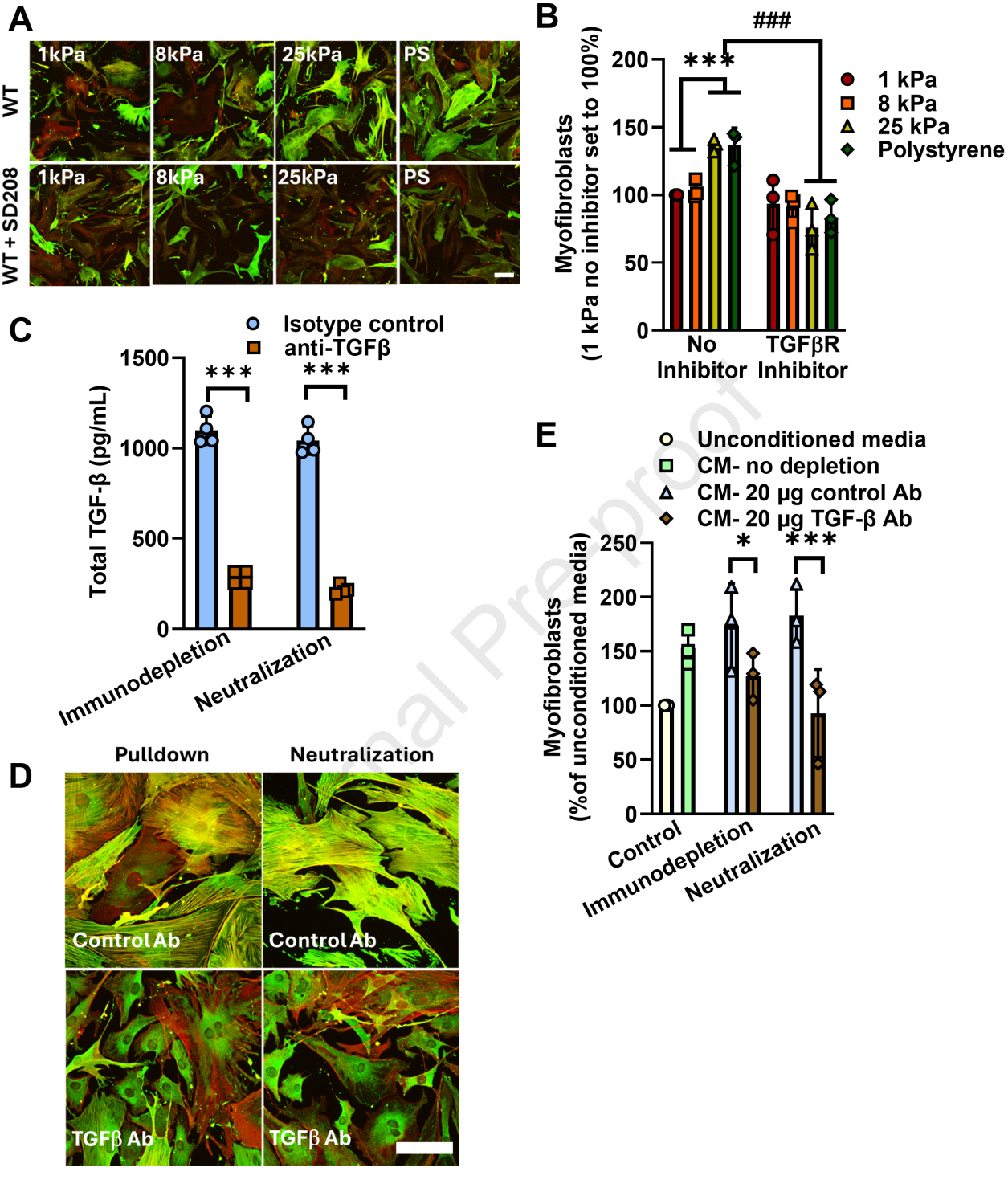
A
WT
WT + SD208
1kPa
8kPa
25kPa
PS
B
Myofibroblasts
(1 kPa no inhibitor set to 100%)
***
###
1 kPa
8 kPa
25 kPa
Polystyrene
No Inhibitor
TGFβR Inhibitor
C
Isotype control
anti-TGFβ
Total TGF-β (pg/mL)
Immunodepletion
Neutralization
D
Pulldown
Neutralization
Control Ab
TGFβ Ab
E
Unconditioned media
CM- no depletion
CM- 20 µg control Ab
CM- 20 µg TGF-β Ab
Myofibroblasts
(%of unconditioned media)
Control
Immunodepletion
Neutralization

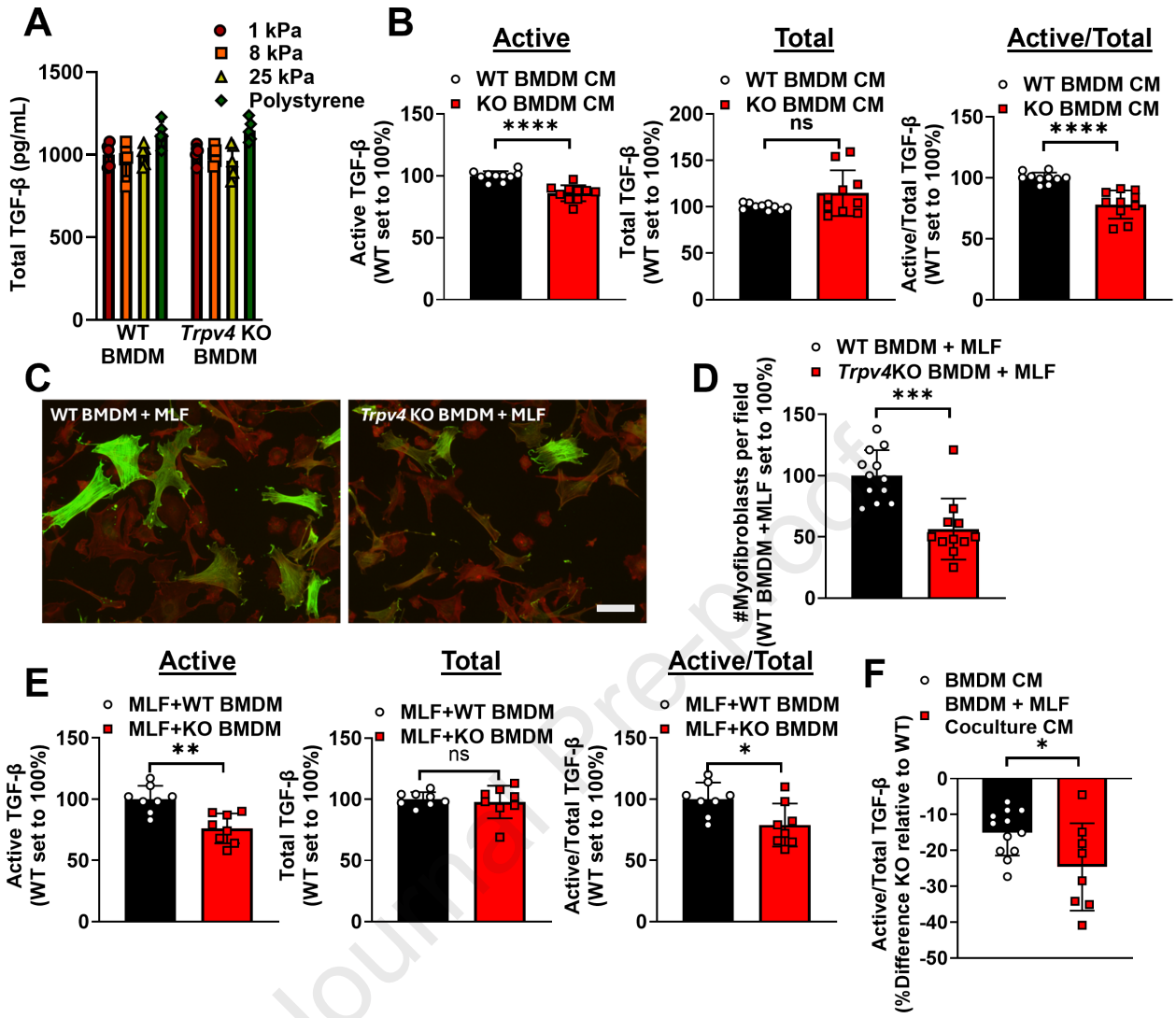

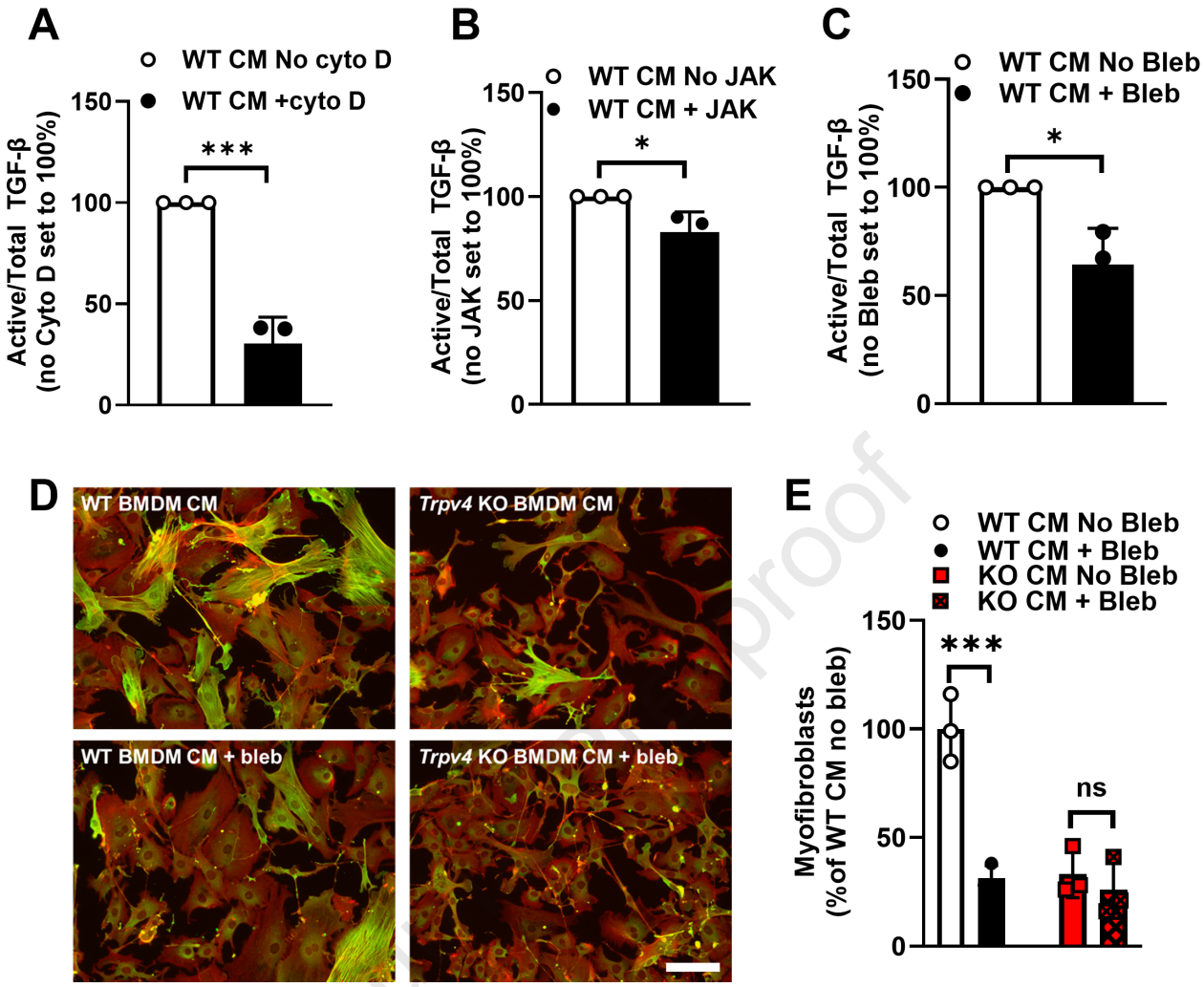

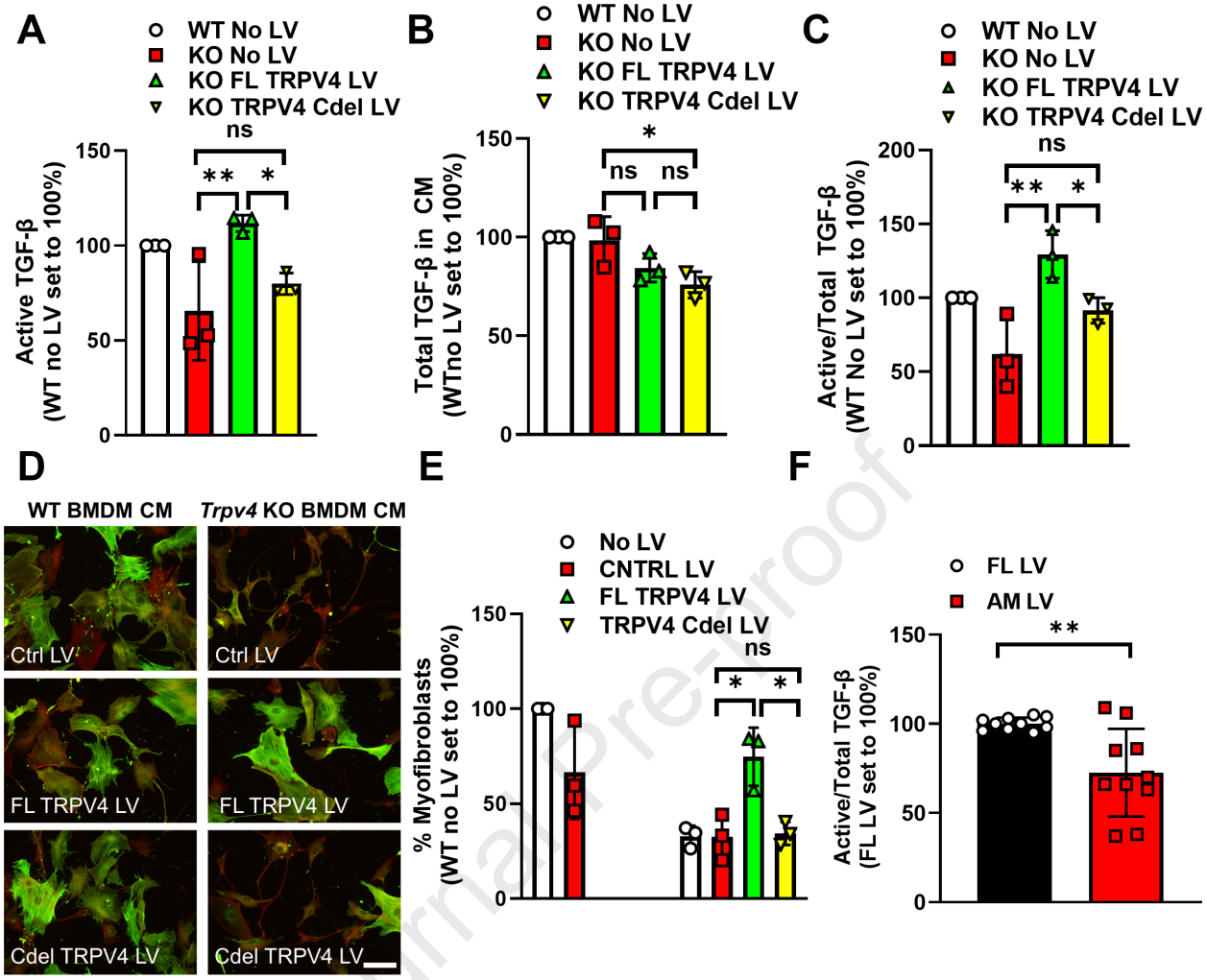

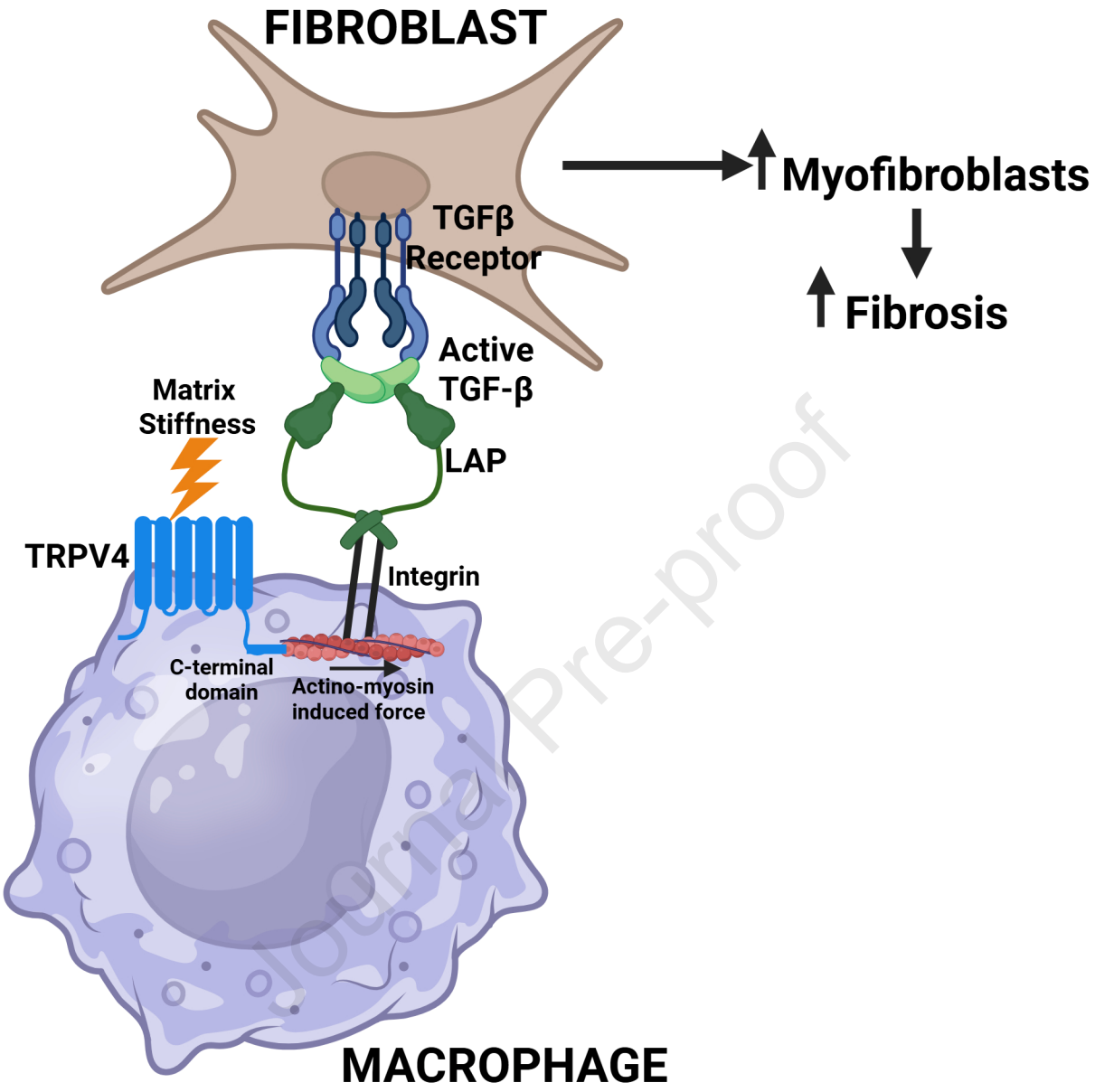

Lisa Grove: Conceptualization, Methodology, Writing-Original Draft, Formal Analysis, Investigation, Data curation. **Caitlin Snyder**: Formal Analysis, Investigation, Data curation. **Adam Boulton**: Visualization, Investigation. **Hongxia Mao***:* Data curation. **Susamma Abraham**: Data curation **Haley Ricci:** Data curation. **Erica Orsini:** Data curation, Writing- Review & Editing. **Brian Southern:** Writing- Review & Editing. **Mitchell Olman**: Conceptualization, Methodology, Writing- Review & Editing, Funding acquisition. **Rachel G. Scheraga:** Conceptualization, Methodology, Formal Analysis, Investigation, Writing-Original Draft, Review & Editing, Supervision, Funding acquisition

Declaration of Interest Statement

☒ The authors declare that they have no known competing financial interests or personal relationships that could have appeared to influence the work reported in this paper.

☐ The author is an Editorial Board Member/Editor-in-Chief/Associate Editor/Guest Editor for this journal and was not involved in the editorial review or the decision to publish this article.

☐ The authors declare the following financial interests/personal relationships which may be considered as potential competing interests:

Declaration of interests

☐ The authors declare that they have no known competing financial interests or personal relationships that could have appeared to influence the work reported in this paper.

☒ The authors declare the following financial interests/personal relationships which may be considered as potential competing interests:

Rachel Scheraga reports financial support was provided by National Institute of Health. If there are other authors, they declare that they have no known competing financial interests or personal relationships that could have appeared to influence the work reported in this paper.